


 Cite this: *RSC Adv.*, 2021, **11**, 33626

Ca(OH)₂-mediated activation of peroxyomonosulfate for the degradation of bisphenol S†

 Leliang Wu,^a Yiting Lin,^a Yimin Zhang,^a Peng Wang,^a Mingjun Ding,^a Minghua Nie,^{ID *ab} Caixia Yan^{*a} and Shiyao Chen^a

Alkaline substances could activate peroxyomonosulfate (PMS) for the removal of organic pollutants, but relatively high alkali consumption is generally required, which can cause too high pH of the solution after the reaction and lead to secondary pollution. Within this study, PMS activated by a relatively low dosage of Ca(OH)₂ (1 mM) exhibited excellent efficiency in the removal of bisphenol S (BPS). The pH of the solution declined to almost neutral (pH = 8.2) during the reaction period and conformed to the direct emission standards (pH = 6–9). In a typical case, BPS was completely degraded within 240 min and followed the kinetics of pseudo-first-order. The degradation efficiency of BPS depended on the operating parameters, such as the Ca(OH)₂, PMS and BPS dosages, initial solution pH, reaction temperature, co-existing anions, humic acid (HA), and water matrices. Quenching experiments were performed to verify that singlet oxygen (¹O₂) and superoxide radicals (O₂^{•-}) were the predominant ROS. Degradation of BPS has been significantly accelerated as the temperature increased. Furthermore, degradation of BPS could be maintained at a high level across a broad range of pH values (5.3–11.15). The SO₄²⁻, NO₃⁻ did not significantly impact the degradation of BPS, however, both HCO₃⁻ and HA inhibited oxidation of BPS by the Ca(OH)₂/PMS system, and Cl⁻ had a dual-edged sword effect on BPS degradation. In addition, based on the 4 identified intermediates, 3 pathways of BPS degradation were proposed. The degradation of BPS was lower in domestic wastewater compared to other natural waters and ultrapure; nevertheless, up to 75.86%, 77.94% and 81.48% of BPS was degraded in domestic wastewater, Yaohu Lake water and Poyang Lake water, respectively. Finally, phenolic chemicals and antibiotics, including bisphenol A, norfloxacin, lomefloxacin hydrochloride, and sulfadiazine could also be efficiently removed via the Ca(OH)₂/PMS system.

Received 9th July 2021
 Accepted 20th September 2021
 DOI: 10.1039/d1ra05286a
rsc.li/rsc-advances

1 Introduction

Bisphenols, a large group of compounds which contain two phenol rings, have been extensively adopted in the manufacture of polycarbonate plastics, phenolic and epoxy resins.¹ Bisphenol A (BPA) is the most widely used bisphenol compound with more than 4.5 million tons produced each year. However, BPA has been restricted in its products and applications in many countries over the past few decades, since it was found to display potential endocrine disruption activity in human and animals. Bisphenol S (BPS) had been developed as a “safe BPA substitution” for replacing BPA,² which inevitably led to the leakage of

this substance into the environment. BPS has a shorter half-life than BPA in water and sediment, and a reduced biodegradability.³ However, BPS exhibits similar toxicological effects (genotoxicity and cytotoxicity) as BPA, but it showed stronger estrogenic activity than BPA.⁴ As the demand for BPS increased, BPS has been frequently detected in surface water and soils and whose concentration (geometric mean: 0.181 mg g⁻¹) was almost as high as that BPA,⁵ which raised potential risk on ecosystems and human health. Unfortunately, numerous treatment processes, including adsorption, coagulation and biodegradation cannot effectively eliminate BPS from water.^{2,3,6} Therefore, it is crucial to develop reliable methods with higher BPS removal efficiencies.

Advanced oxidation processes (AOPs) have been extensively applied promising technologies for the degradation of recalcitrant organic pollutants. In particular, hydrogen peroxide (H₂O₂), peroxyomonosulfate (PMS) and persulfate (PS) based AOPs have attracted wide attention. Compared to H₂O₂ and PS, the PMS is easier to activate due to its dissymmetric structure and shorter length of the O–O bond. In general, PMS can be

^aSchool of Geography and Environment, Key Laboratory of Poyang Lake Wetland and Watershed Research, Ministry of Education, Jiangxi Normal University, Nanchang 330022, China. E-mail: mhnie@jxnu.edu.cn; wysycx@foxmail.com

^bKey Laboratory of Eco-geochemistry, Ministry of Natural Resource, Beijing 100037, China

† Electronic supplementary information (ESI) available. See DOI: [10.1039/d1ra05286a](https://doi.org/10.1039/d1ra05286a)



activated by heat, ultrasonic, and transition metal catalysis.^{7–9} However, these methods were limited to be widely applied due to the high energy-input or metal leaching problems. Therefore, environmentally friendly approaches for the effective removal of organic pollutants are highly desirable.

Recently, alkaline substances, including borate and Na_2CO_3 have been confirmed to efficiently activate PMS to generate reactive oxygen species (ROS).^{10,11} The previous study had shown that acid orange 7, BPA and acetaminophen in water could be efficiently removed by PMS at alkaline conditions.^{12,13} However, the methods of PMS activation by alkaline substances have shown some drawbacks. Such as, after the reacts of alkali activated PMS system, the pH of solution was generally too high and cannot be directly discharged into the actual environment. Secondary treatment undoubtedly would increase the cost of water pollution treatment. Therefore, it is urgent to optimize this method by adjusting the dosages of alkaline substances to change the pH of solution after reaction to reach the ideal value.

$\text{Ca}(\text{OH})_2$ is also a kind of high-performance alkali reagent used in wastewater treatments. Compared with NaOH (263.16 USD per Ton), borate (727.62 USD per Ton) and Na_2CO_3 (294.14 USD per Ton), $\text{Ca}(\text{OH})_2$ has distinct advantages because of a lower price (77.41 USD per Ton). Therefore, in the present study, the economic $\text{Ca}(\text{OH})_2$ was chosen as an activator of PMS for the degradation of BPS. The amount of $\text{Ca}(\text{OH})_2$ was strictly controlled to ensure that the solution pH after reaction meets to 6–9. Besides, this study intended to explore the degradation of BPS in the $\text{Ca}(\text{OH})_2$ /PMS system under various experimental conditions (including $\text{Ca}(\text{OH})_2$, PMS and BPS dosages, co-existing anions and HA, initial solution pH and temperature, etc.). In addition, the dominant ROS in the $\text{Ca}(\text{OH})_2$ /PMS system were identified. Furthermore, it also studied the degradation of BPS in the different water matrices and the application to other pollutions. Moreover, the reaction products and the transformation pathways of BPS were also proposed.

2 Materials and methods

2.1 Materials

BPS, PMS, PS, BPA, H_2O_2 , furfuryl alcohol (FFA), thiampenicol (TAP), lomefloxacin hydrochloride (LOM), enrofloxacin (ENR), and norfloxacin (NOR), were purchased from Aladdin Chemicals Co. (China). $\text{Ca}(\text{OH})_2$, NaCl , $\text{NaH}_2\text{PO}_4 \cdot 2\text{H}_2\text{O}$, NaNO_3 , NaHCO_3 , NaOH , H_2SO_4 , Na_2SO_4 , ethanol (EtOH), *tert*-butyl alcohol (TBA), ascorbic acid (AA) and *L*-histidine (*L*-his), nitro blue tetrazolium (NBT) and *p*-benzoquinone (BQ) were obtained from Sinopharm (China). Humic acid (HA) was purchased from Xiya Reagent Co. (China). Methanol (EtOH) was supplied by CNW Technologies GmbH (Germany). All chemical reagents were at least of analytical grade or higher purity. Ultrapure water with a resistivity of $18.2 \text{ M}\Omega \text{ cm}^{-1}$ produced from a water purification system was used to prepare all solutions.

2.2 Experimental procedure

Except for the influence of the reaction temperature, all degradation experiments were carried out at a constant temperature

($25.0^\circ\text{C} \pm 0.5^\circ\text{C}$) controlled by a thermostat water bath. In detail, a specific aliquot of BPS and other chemicals substance stock solution were transferred into a 40 mL brown glass bottle, followed by the addition of designated volumes of $\text{Ca}(\text{OH})_2$ and PMS, then approximately 1 mL of the reaction solution in a bottle at predetermined time intervals and detected by HPLC. The experiments for the removal of BPA, TAP, NOF, LOM and ENR were carried out under identical conditions. To investigating the influence of the initial pH, the initial pH of the solution was adjusted to a specific pH by using 0.1 M H_2SO_4 and 0.1 M NaOH solution. For verifying the application of the $\text{Ca}(\text{OH})_2$ /PMS system in actual water, four different water samples were collected, including Poyang Lake water (the largest freshwater lake of China), Yaohu Lake water, tap water, and domestic water (collected from a university campus). All the above water samples were filtered through 0.45 μm filters before the experiment, the detailed physicochemical properties of these water types are shown in Table S1.[†] 1.5 mM PMS and 1 mM $\text{Ca}(\text{OH})_2$ were added to the real water samples for experiment.

In order to identify the contribution of ROS in BPS degradation by the $\text{Ca}(\text{OH})_2$ /PMS system, different ROS quenchers were added. AA (5 mM and 10 mM) as ROS scavenger, EtOH (10 mM and 100 mM) as both HO^\cdot and $\text{SO}_4^{\cdot-}$ scavengers, TBA (10 mM and 100 mM) as HO^\cdot scavenger, *L*-His (5 mM and 10 mM) and NBT (0.02 mM, 0.05 mM and 0.1 mM) were employed to eliminate $^1\text{O}_2$ and $\text{O}_2^{\cdot-}$, respectively. All reactions were independently performed in at least triplicate and the values with the standard deviations were presented in figures.

2.3 Analytical methods

The concentrations of BPS, BPA, TAP, ENR, NOR and LOM were measured by high-performance liquid chromatography (HPLC, 1260 II, Agilent, USA) equipped with an Athena C18 column (150 mm \times 2.1 mm, 5 μm). Detailed HPLC parameters for target organic compounds analysis were shown in Table S2.[†] The remaining concentration of PMS in the solution was determined by iodometry.¹⁴ The pH values were measured with a pH-3C pH meter (Shanghai Lei Co., Ltd.). The concentration of NBT was measured at a fixed wavelength ($\lambda_{\text{NBT}} = 259 \text{ nm}$) by a UV-3300 UV-vis spectrophotometer (Mapada Inc., Shanghai, China).

The intermediated products were identified by using a liquid chromatography-time-of-flight mass spectrometer (LC-TOF-MS, Xevo G2-XS Qtof, Waters, USA) equipped with an ACQUITY UPLC BEHC18 Column (2.1 mm \times 100 mm, 1.7 μm). The column temperature was 40°C , and the mobile phase consisted of acetonitrile (40%) and 0.1% formic acid in water (60%) with a 0.4 mL min^{-1} flow rate, and the injection volume was $10 \mu\text{L}$. The mass spectra were measured with a scan range of 100–2000 Da in a positive mode.

The percentage of compounds remaining were calculated according to eqn (1):

$$\text{Degradation (\%)} = \frac{C_t}{C_0} \times 100\% \quad (1)$$



where C_0 is the initial compounds concentration, and C_t is the compounds concentration at time t min in the $\text{Ca}(\text{OH})_2/\text{PMS}$ system.

3 Results and discussion

3.1 Degradation efficiency of BPS in different systems

The performances of different systems on the degradation of 20 μM BPS within 240 min were shown in Fig. 1. No remarkable removal of BPS was observed in the presence of $\text{Ca}(\text{OH})_2$ alone, which means that $\text{Ca}(\text{OH})_2$ could not directly react with BPS. PMS is a strong oxidant and can directly oxidize tetracyclines.¹⁵ However, only 3.57% of BPS was degraded in the single PMS system, which was attributed to the oxidative properties of PMS. In contrast, BPS was almost completely degraded in the $\text{Ca}(\text{OH})_2/\text{PMS}$ system. These results showed that both PMS and $\text{Ca}(\text{OH})_2$ were indispensable for the degradation of BPS. The fitting line between $\ln([C_t/C_0])$ and reaction time was showed a good linearity ($R^2 = 0.995$), which indicated that the degradation of BPS was well fitted by the pseudo-first-order kinetic model, and the rate constant (k_{obs}) value was 0.0201 min^{-1} . Compared with the $\text{Ca}(\text{OH})_2/\text{PMS}$ system, the $\text{Ca}(\text{OH})_2/\text{PS}$ and $\text{Ca}(\text{OH})_2/\text{H}_2\text{O}_2$ had no obvious effect on BPS. It could be interpreted that the PMS has an asymmetric molecular structure on both sides of the peroxide bond ($-\text{O}-\text{O}-$) inside compared to the PS and H_2O_2 ,¹⁶ which led to PMS can more easily be activated by $\text{Ca}(\text{OH})_2$.

The pH was also monitored as the reaction processes. As shown in Table R3,[†] the solution pH after the addition of solid PMS dropped to 3.96, the decline of pH was due to large number of H^+ produced by PMS dissolved in solution. However, the pH of solution increased to 9.69 with the addition of $\text{Ca}(\text{OH})_2$ and finally decreased to 8.20 within 240 min, this phenomenon may be attributed to acidic intermediate products formed. Fortunately, the pH complied with the direct emission standards (6–9) after reaction. It is convenient to practical wastewater treatment without additional pH adjustment.

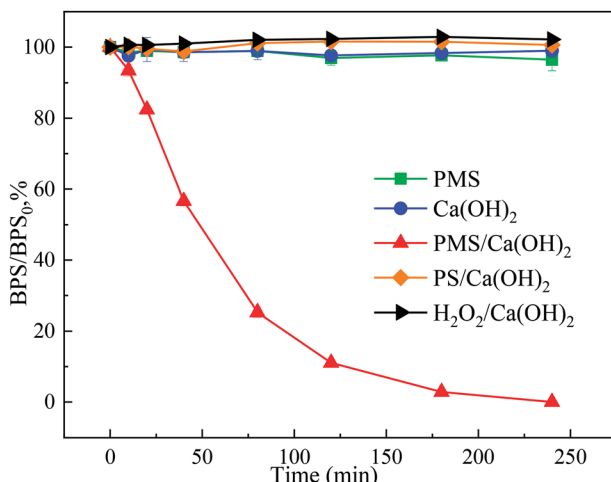


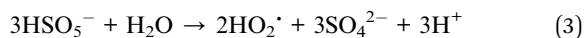
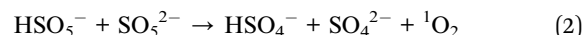
Fig. 1 Degradation efficiency of BPS in the different systems, $[\text{Ca}(\text{OH})_2] = 1 \text{ mM}$, $[\text{PMS}]_0 = [\text{PS}]_0 = [\text{H}_2\text{O}_2]_0 = 1.5 \text{ mM}$, $[\text{BPS}]_0 = 20 \mu\text{M}$.

3.2 ROS identification and possible mechanism of PMS activation

$\text{Ca}(\text{OH})_2$ showed excellent performance in PMS activation for BPS degradation. It is necessary to investigate the PMS activation mechanism by $\text{Ca}(\text{OH})_2$. Scavenging experiments were used to elucidate the potential involvement of ROS in the $\text{Ca}(\text{OH})_2/\text{PMS}$ system (Fig. 2). As a well-known ROS quencher strongly, AA prohibited the degradation of BPS as shown in Fig. 2(a),¹⁷ which suggested that ROS playing an important role in the degradation of BPS. HO^\cdot and SO_4^{2-} are usually considered to be the main ROS generated in PMS-based AOPs.¹⁸ TBA can efficiently quench HO^\cdot ($k = 6 \times 10^8 \text{ M}^{-1} \text{ s}^{-1}$), whereas the EtOH can efficiently scavenge both HO^\cdot ($k = 1.2-2.8 \times 10^9 \text{ M}^{-1} \text{ s}^{-1}$) and SO_4^{2-} ($k = 1.6-7.7 \times 10^7 \text{ M}^{-1} \text{ s}^{-1}$).¹⁸ With the addition of different concentrations (10 mM and 100 mM) of TBA and EtOH, it was observed that EtOH and TBA have no inhibition effect to the degradation of BPS, indicating that neither HO^\cdot nor SO_4^{2-} were main ROS involved in the $\text{Ca}(\text{OH})_2/\text{PMS}$ system.

Singlet oxygen (${}^1\text{O}_2$) and superoxide radicals (O_2^\cdot) were also proposed to be formed in the PMS activation. L-his is the scavenger of ${}^1\text{O}_2$ ($k = 3.2 \times 10^7 \text{ M}^{-1} \text{ s}^{-1}$), as shown in Fig. 2(b), the degradation of BPS was intensely inhibited with the addition of L-his, which implied that ${}^1\text{O}_2$ played an essential role in the removal of BPS. NBT was commonly used as a scavenger to trap O_2^\cdot ($k = 5.88 \times 10^4 \text{ M}^{-1} \text{ s}^{-1}$).²⁰ With the addition of NBT (0.02 mM, 0.05 mM and 0.1 mM), the degradation of BPS was slightly suppressed and decreased from 100% to 92.58%, 93.37% and 92.88%, which implied that O_2^\cdot also participated in the reaction. According to the above-obtained results, the possible activation mechanism of PMS by $\text{Ca}(\text{OH})_2$ was proposed as follows:

Previous literature proposed that ${}^1\text{O}_2$ could be slowly generated by self-decomposition of PMS (eqn (2)).¹⁹ Besides, under the alkaline conditions, $\text{Ca}(\text{OH})_2$ activated PMS generates HO_2^\cdot (eqn (3)), HO_2^\cdot would quickly decompose into O_2^\cdot (eqn (4)). Furthermore, O_2^\cdot generated might be recombined and ${}^1\text{O}_2$ and H_2O_2 were formed based on eqn (5). Moreover, H_2O_2 would also generate ${}^1\text{O}_2$ by disproportionation reaction.¹¹ It is worth mentioning that hydrogen ions were continuously generated during reaction, which is also the reason that the pH of solution dropped after reaction.



Additionally, to further confirm the generation of O_2^\cdot and ${}^1\text{O}_2$ in $\text{Ca}(\text{OH})_2/\text{PMS}$ system, the selected probe chemical FFA (1 mM) and NBT (1 mM) were employed to detect ${}^1\text{O}_2$ and O_2^\cdot , respectively. As shown in Fig. S1,[†] the concentration of FFA and NBT decreased as the reaction proceeds. Which implied both



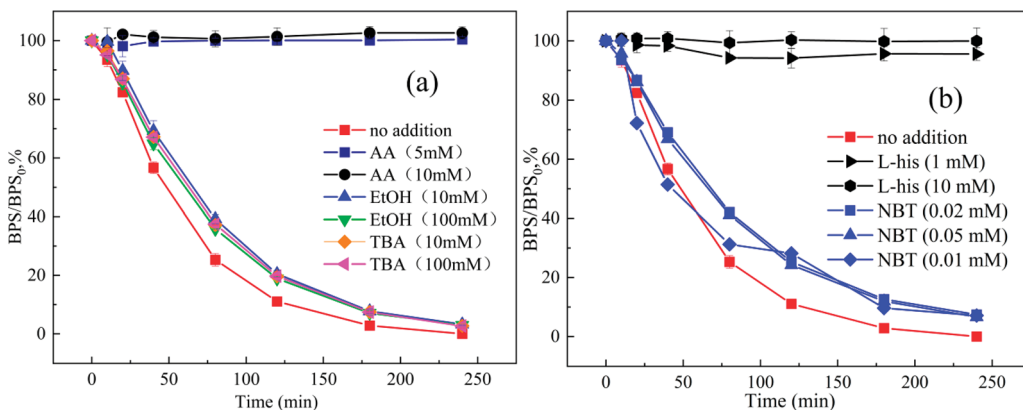


Fig. 2 Effect of AA, EtOH, TBA (a) and L-his, NBT (b) on BPS removal, $[\text{Ca}(\text{OH})_2]_0 = 1 \text{ mM}$, $[\text{PMS}]_0 = 1.5 \text{ mM}$, $[\text{BPS}]_0 = 20 \mu\text{M}$.

$^1\text{O}_2$ and $\text{O}_2^{\cdot-}$ were involved in the $\text{Ca}(\text{OH})_2/\text{PMS}$ system, and $^1\text{O}_2$ played the major role, the $\text{O}_2^{\cdot-}$ maybe served as the crucial precursor in the formation of $^1\text{O}_2$.

3.3 Degradation of BPS by the $\text{Ca}(\text{OH})_2/\text{PMS}$ system

3.3.1 Influence of $\text{Ca}(\text{OH})_2$ concentration. Fig. 3(a) showed that BPS degradation efficiencies with fixed concentration (1.5 mM) of PMS using different $\text{Ca}(\text{OH})_2$ concentrations (0–2.0 mM). Only 3.70% of BPS were degraded within 240 min in the presence of 0.25 mM $\text{Ca}(\text{OH})_2$, which might be attributed to the unfavorable for PMS activation under low pH condition ($\text{pH} =$

3.66), PMS hardly decomposes to produce ROS under acidic conditions. When the concentrations of $\text{Ca}(\text{OH})_2$ were further increased from 0.5 mM to 1 mM, the degradation of BPS increased from 6.42% to 100%. However, when the concentrations were further increased to 1.5 mM and 2 mM, the degradation of BPS were decreased to 82.17% and 38.17%, respectively. A similar trend was also reported in the polyphosphates/PMS process for AO7 degradation.²¹

The concentrations of $\text{Ca}(\text{OH})_2$ play an important in affecting the pH of solution. So, the pK_a value of BPS and PMS should be considered. The pK_a value of BPS is 8.2,²² therefore,

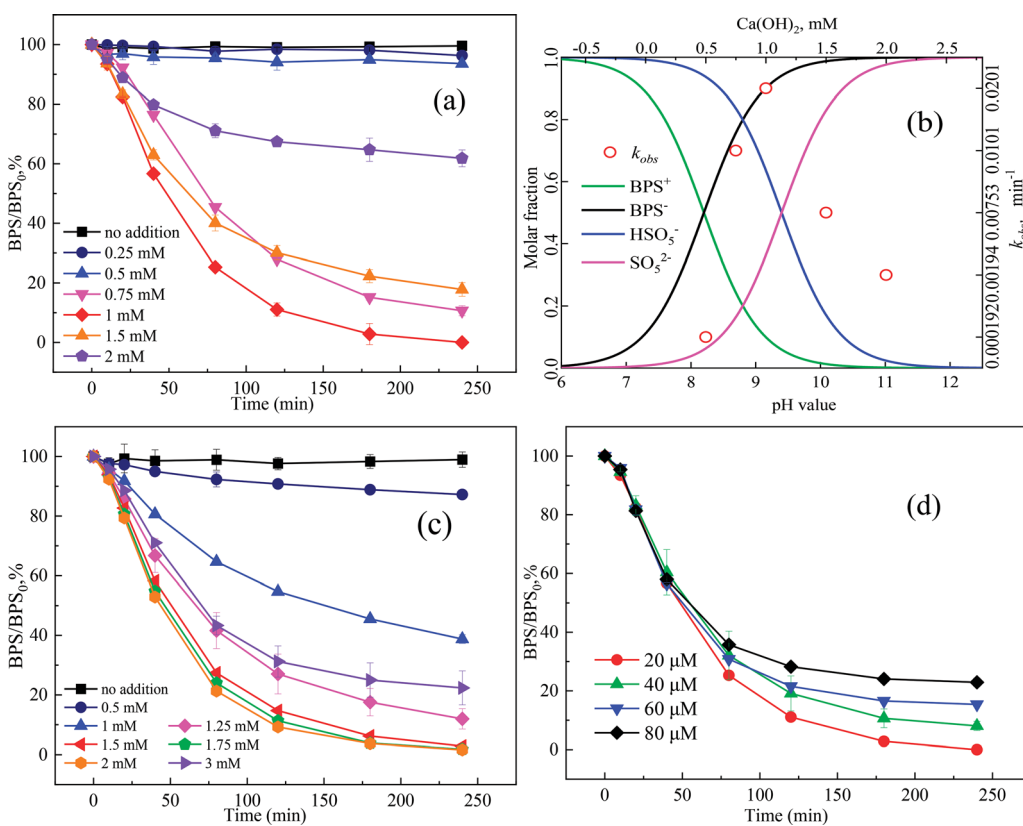


Fig. 3 Removal rate of BPS under different initial $\text{Ca}(\text{OH})_2$ concentrations (a), the species of both BPS and PMS in different pH values and changes of k_{obs} under different initial $\text{Ca}(\text{OH})_2$ concentrations (b), removal rate of BPS under initial different PMS concentrations (c), the effect of removal rate of BPS at the different BPS concentrations (d), $[\text{Ca}(\text{OH})_2]_0 = 0\text{--}2 \text{ mM}$, $[\text{PMS}]_0 = 0\text{--}3 \text{ mM}$, $[\text{BPS}]_0 = 20\text{--}80 \mu\text{M}$.



BPS mainly exists in the deprotonated form (BPS^-) when the pH > 8.2 , and in the protonated form (BPS^+) when pH < 8.2 (Fig. 3(b)). Meanwhile, the $\text{p}K_a$ value of PMS is 9.4, PMS is mainly existing in the form of SO_5^{2-} when the pH > 9.4 , and in the form of HSO_5^- when the pH < 9.4 .²³ In addition, the obtained degradation rate constant (k_{obs}) for BPS with different initial $\text{Ca}(\text{OH})_2$ concentrations was as follows: 0.00019 min^{-1} ($\text{Ca}(\text{OH})_2$ 0.5 mM, pH 8.03) $< 0.00194 \text{ min}^{-1}$ ($\text{Ca}(\text{OH})_2$ 2 mM, pH 10.96) $< 0.00753 \text{ min}^{-1}$ ($\text{Ca}(\text{OH})_2$ 1.5 mM, pH 10.89) $< 0.01010 \text{ min}^{-1}$ ($\text{Ca}(\text{OH})_2$ 0.75 mM, pH 9.24) $< 0.02010 \text{ min}^{-1}$ ($\text{Ca}(\text{OH})_2$ 1 mM, pH 9.69). The k_{obs} value at pH = 9.69 (1 mM $\text{Ca}(\text{OH})_2$) was at least 104 times compared to the k_{obs} value at pH = 8.03 ($\text{Ca}(\text{OH})_2$ 0.5 mM), and the k_{obs} value tended to increase with increasing fraction of SO_5^{2-} but decreased as the increasing fraction of BPS^- . This may be attributed to PMS could generate ROS according to eqn (2)–(6), and PMS decomposed quicker at higher solution pH. However, electrostatic repulsion would be stronger as the increase of SO_5^{2-} and BPS^- concentration, which might result in the decrease of BPS degradation.²⁴ All these indicated that BPS degradation by $\text{Ca}(\text{OH})_2$ /PMS system exhibited a significant pH dependence, so it is very important to control the dosages of $\text{Ca}(\text{OH})_2$.

3.3.2 Influence of PMS concentration. As shown in Fig. 3(c), the effect of different concentrations of PMS on the BPS degradation was also investigated. PMS generally exhibited a positive effect on the target organic contaminant degradation in the $\text{Ca}(\text{OH})_2$ /PMS system. The degradation of BPS increased from 12.79% to 61.23%, 88.03% and 100%, respectively, as the PMS concentration increased from 0.5 mM to 1 mM, 1.25 mM and 1.5 mM. However, when the PMS concentration continued to increase to 1.75 mM, 2 mM and 3 mM, the BPS degradation significantly decreased to 98.21%, 98.39% and 77.63%, respectively. PMS is the source of ROS, and a certain extent more PMS means more ROS generated.²⁵ Whereas, as the initial concentration of PMS continues increased, the degradation rate of BPS declined instead, the reason may be due to the high PMS concentration in the $\text{Ca}(\text{OH})_2$ /PMS system resulted self-quenching of ROS, and the generation of low-activity species (SO_5^{2-}),²⁶ then influenced the degradation of BPS. Furthermore, the solution pH decreased to 7.65 with the addition of 3 mM PMS. As illustrated in Section 3.3.1, it was unfavorable for PMS activation in the $\text{Ca}(\text{OH})_2$ /PMS system when the solution pH was lower than 9.4, thus the dominating role responsible for BPS degradation shifts to the primary solution pH. Given the mentioned issues, 1.5 mM of PMS was chosen for further experiment in the present study.

3.3.3 Influence of PMS adding mode. For further improvement of the oxidation efficiency, the adding mode of PMS was also studied. A total of 1.5 mM PMS was divided equally into n portions ($n = 1, 2, 3, 5$), which were added sequentially with equal intervals within 240 min as shown in Fig. S2.† With the addition number increased from 1 to 5, the degradation of BPS was decreased from 100% to 77.94%, and the k_{obs} was slowed down from 0.0201 min^{-1} to 0.00397 min^{-1} . Such a change showed that increasing the addition number of PMS could not result in higher BPS degradation. However, there be reported that the sequential addition of PMS resulted in

accelerating the removal of pollutions.²⁷ Compared with metal catalysts, PMS activated by $\text{Ca}(\text{OH})_2$ usually consistent and less aggressive because of the slow generation rate of ROS.²⁸ Less addition number of PMS resulted in higher initial PMS dosages in solution, more ROS would be generated and available for the oxidation of BPS, which led to the higher BPS degradation.

3.3.4 Influence of initial BPS concentration. As shown in Fig. 3(d), it was apparent that the efficiency of BPS degradation decreased from 100% to 77.08% with the initial BPS dosages increasing from 20 μM to 80 μM . The continuous consumption of quantitative oxidant (1.5 mM PMS) led to the incomplete removal of high BPS dosages. The k_{obs} for BPS degradation were from 0.02010 min^{-1} to 0.00660 min^{-1} with the initial BPS dosages from 20 μM to 80 μM . The decrease in BPS degradation could probably be explained by the fact that the amount of ROS generated at a given PMS concentration was identical. The continuous consumption of quantitative ROS (1.5 mM PMS) caused the incomplete removal of high BPS concentrations.²⁹ At higher initial BPS dosages, the lower ratio of ROS to BPS provided less probability for BPS molecules being attacked by ROS, which led to lower k_{obs} values.³⁰ In addition, as the initial concentration of BPS increased, degradation products would also increase, which increased the competition for ROS.

3.4 Influence of solution temperature

Effect of different reaction temperatures (5 °C, 25 °C, 40 °C, and 50 °C) on the degradation of BPS by the $\text{Ca}(\text{OH})_2$ /PMS system were investigated (Fig. 4(a)). It was obvious that temperature had a strong influence on the oxidation of BPS. With temperature increased from 5 °C to 25 °C, 40 °C, and 50 °C, BPS degradation was significantly accelerated and the rate climbed from 0.00240 min^{-1} to 0.20100 min^{-1} , 0.21100 min^{-1} , and 0.59230 min^{-1} , respectively. This phenomenon could be interpreted for the following reason: as temperature increased, the rate of ROS formation was quicker. In addition, the thermal movement of molecules accelerated and the collision probability between molecules increased, thus speeding up the degradation of BPS.^{31,32} Moreover, the k_{obs} values had a good correlation with the reaction temperature. And the apparent activation energy E_a value for BPS degradation in the $\text{Ca}(\text{OH})_2$ /PMS system was 90.71 kJ mol⁻¹ according to Arrhenius equation (eqn (7)),³³ These results were similar to HPO_3^{2-} /PMS system removal AO7 (94.4 kJ mol⁻¹).³⁴ The low activation energy implied that the $\text{Ca}(\text{OH})_2$ /PMS system was promising for heterogeneous catalytic reactions.

$$\ln(k_{\text{obs}}) = \ln(A) - \frac{E_a}{R} \left(\frac{1}{T} \right) \quad (7)$$

where A represents the pre-exponential factor, E_a represents the activation energy for the reaction (J mol⁻¹), and R represents molar gas constant (8.314 J mol⁻¹ K⁻¹), T represents absolute temperature (K).

3.5 Influence of initial solution pH

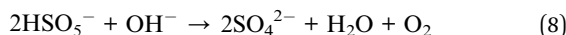
Solution pH affect the oxidation of the target compounds by altering the speciation of both substrate and oxidant. Therefore,



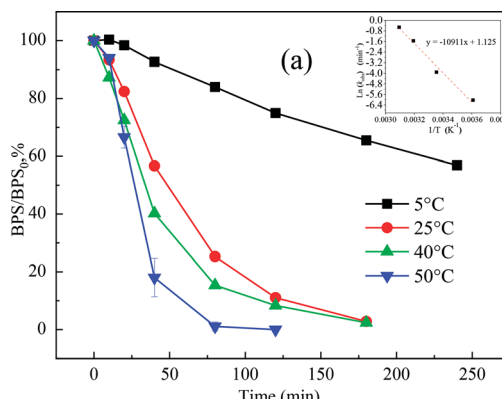
initial solution pH usually significantly influences the performance of AOPs in water. Effect of initial solution pH on the removal of BPS was investigated under a series of initial pH conditions ($\text{pH} = 3.19\text{--}11.15$) with the results illustrated in Fig. 4(b). The degradation of BPS was only 14.27% and the k_{obs} was 0.00678 min^{-1} when the initial pH of solution was 3.19, which probably due to the oxidation reaction was ineffective under acidic conditions ($\text{pH} < 5$) in the $\text{Ca}(\text{OH})_2/\text{PMS}$ system. Under acidic conditions, the formation of a strong H-bond between H^+ and the O-O bond in PMS was dominated thus inhibited ROS generation.³⁵

As the initial pH changed to 5.30, 7.01 and 9.39, the degradation of BPS degradation increased to 96.50%, 98.03% and 97.62%, respectively, and the k_{obs} was resumed to 0.01400 min^{-1} , 0.01670 min^{-1} and 0.01530 min^{-1} , respectively. After the addition of $\text{Ca}(\text{OH})_2$, the pH of the solution immediately increased from 5.30, 7.01 and 9.39 to 9.44, 10.27 and 10.77, respectively. As interpreted in Section 3.3.1, PMS existed mainly in SO_5^{2-} when solution pH was higher than 9.4. Therefore, more ${}^1\text{O}_2$ could be generated according to eqn (2)–(6), which allowed BPS to be efficiently degraded. The final pH dropped slightly to 7.64, 9.56 and 9.73, respectively, which was probably due to the decomposition of PMS and the formation of small molecular-weight organic acids as the intermediates of BPS.¹⁰

However, when the initial solution pH increased to 11.15, and the final solution pH value dropped to 10.26, the rate of BPS degradation reduced to 63.80% with the k_{obs} decreased to 0.00425 min^{-1} . It indicated that the solution pH in the near-neutral or neutral conditions was more favorable to BPS removal than a stronger alkaline condition. It has been reported that the PMS could be self-decomposed to SO_4^{2-} and O_2 according to eqn (8) at high pH values,¹¹ which resulted in a notable decrease in BPS degradation.



Fortunately, the BPS degradation by $\text{Ca}(\text{OH})_2/\text{PMS}$ system efficiency maintained on a high level in a wide range of pH values, which is favorable to its potential application in the treatment of real wastewater.



3.6 Influence of co-existing water matrix

Anions and natural organic matter (NOM) are widespread in natural water matrices, resulting in a complex aquatic environment. These co-existing substances in water may react with ROS and further inhibit the oxidation of BPS.

As showed in Fig. 5(a), the presence of 1 mM Cl^- had slight suppression on BPS degradation, which was similarly observed on the degradation of organic contaminants in PMS-based AOPs.³⁶ Cl^- could be oxidized by ROS to generate chlorine-free radicals (Cl^\cdot , $\text{Cl}_2\cdot^-$) with lower activity, thereby inhibiting the degradation of BPS.³⁷ However, as the concentration of Cl^- further increased to 5 mM and 10 mM, the k_{obs} of BPS were improved from 0.02010 min^{-1} to 0.02530 min^{-1} and 0.02780 min^{-1} , respectively. The accelerated BPS degradation in the presence of Cl^- could be attributed to the production of reactive chlorine (like HOCl and Cl_2) through a two-electron transfer reaction according to eqn (9) and (10).³⁸ Which might participate in the degradation of BPS and accelerated the removal of BPS.

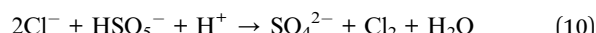
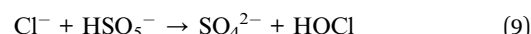


Fig. 5(b) showed the influence of HCO_3^- on BPS removal. The BPS degradation declined to 89.71% in the presence of 1 mM HCO_3^- , and the degradation rate further declined to 67.58% (5 mM HCO_3^-) and 63.83% (10 mM HCO_3^-). According to previous research,³⁹ HCO_3^- would react with PMS to generate HCO_4^- . However, HCO_4^- was erratic, and it would resolve into HCO_3^- and H_2O_2 , which could create an unfavorable condition for BPS degradation (eqn (11) and (12)). Besides, the addition of HCO_3^- would strongly influence solution pH, the solution pH was decreased to 10.16, 9.64 and 9.50 as the dosages of HCO_3^- increased to 1 mM, 5 mM and 10 mM, which would slow the degradation of BPS. In addition, it reported that HCO_3^- could quench ROS to produce less reactive carbonate ones (HCO_3^\cdot and CO_3^{2-}) according to Fig. 5(c) and (d).⁴⁰ the degradation of BPS was not significantly affected with the addition of SO_4^{2-} and

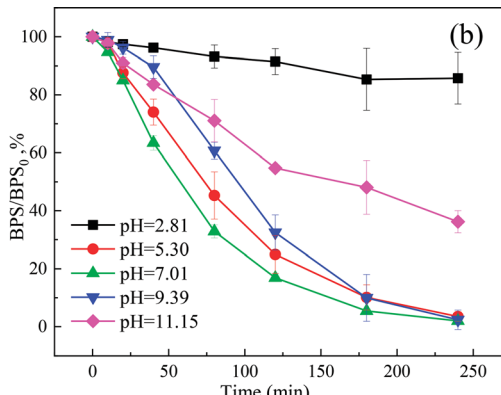


Fig. 4 Removal rate of BPS under different temperatures (a), removal of BPS under different initial pH (b), $[\text{Ca}(\text{OH})_2]_0 = 1 \text{ mM}$, $[\text{PMS}]_0 = 1.5 \text{ mM}$, $[\text{BPS}]_0 = 20 \mu\text{M}$, temperatures = 5–50 °C, pH = 3.19–11.15.



NO_3^- , which implied that both of these two anions don't react with $^1\text{O}_2$ and $\text{O}_2^{\cdot-}$.⁴¹

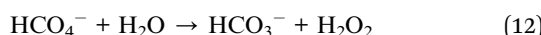


Fig. 5(e) showed the influence of HA on the degradation of BPS. In this study, the degradation of BPS in the presence of 5 mg L^{-1} , 20 mg L^{-1} and 50 mg L^{-1} HA was 98.62% , 96.84% and 96.32% , respectively. As the concentration of HA increased, the degree of inhibition was stronger. Similar trends also appeared in the UV/PMS removal of BPA by UV/PMS system.⁴² HA containing plenty of carboxyl and hydroxyl groups can inhibit the degradation process by quenching radicals and competing with

target contaminants for ROS.⁴³ Nevertheless, the removal efficiency of BPS was higher than 96% in the presence of 50 mg L^{-1} HA, revealing that the $\text{Ca}(\text{OH})_2/\text{PMS}$ system was a promising process for the decontamination of BPS in water even contained a high concentration of HA.

3.7 Pathway of BPS degradation

In the $\text{Ca}(\text{OH})_2/\text{PMS}$ system, BPS was completely degraded and about 60% PMS was consumed within 240 min. Interestingly, PMS was no longer consumed (Fig. 6(a)) after 80 min. It may be due to the pH decreasing gradually as the reaction progress, which was not conducive to the decomposition of PMS. An important indicator of organic removal is the degree of mineralization, which can be determined by the TOC removal.

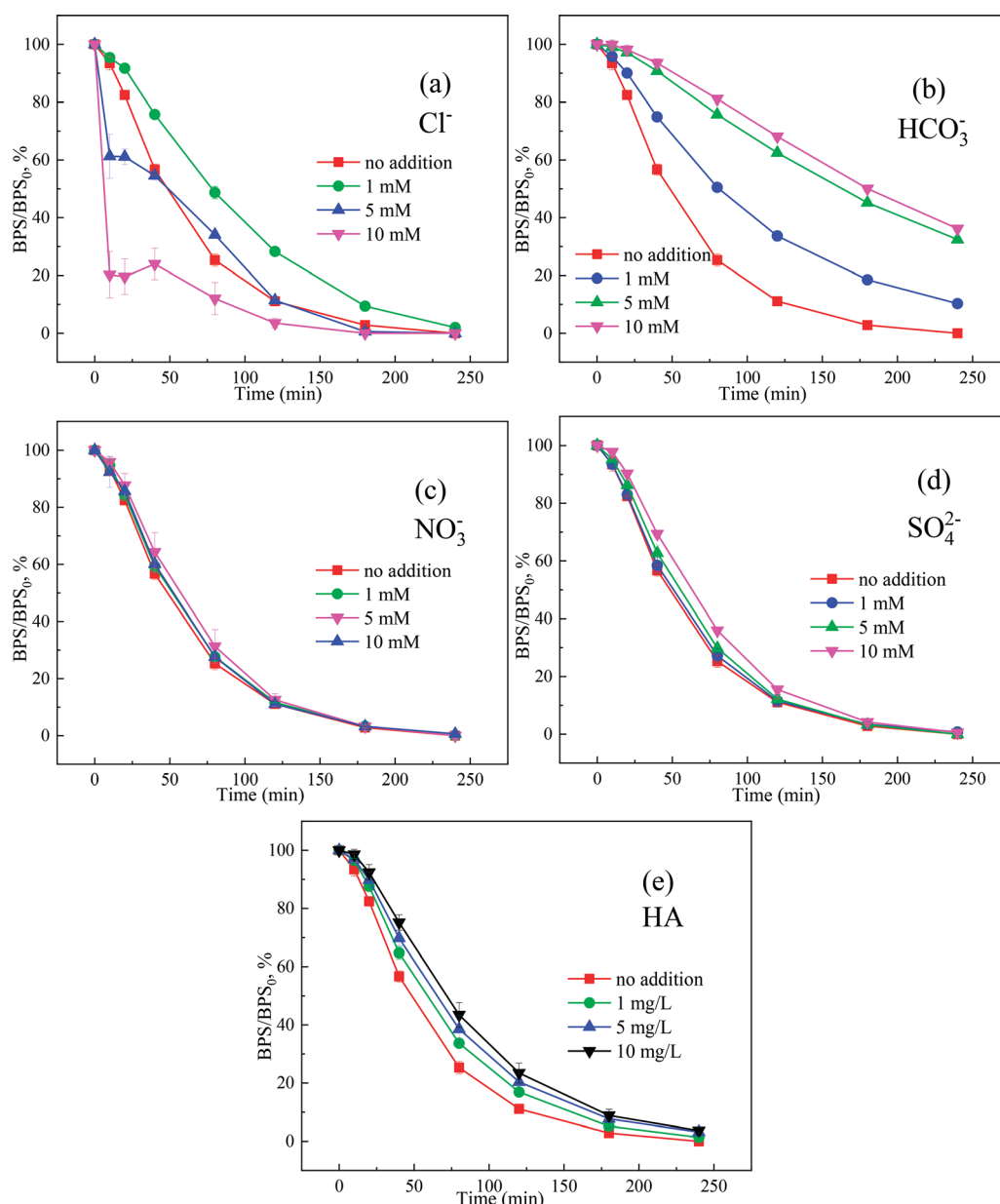
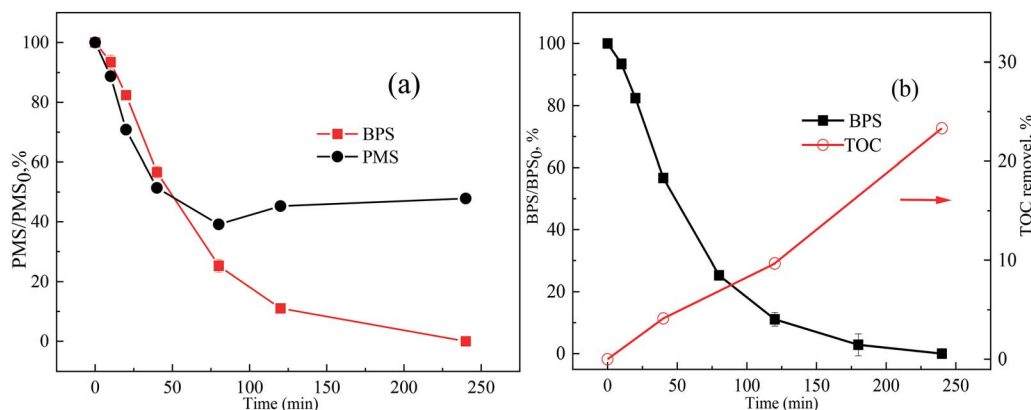


Fig. 5 The effect of Cl^- (a), SO_4^{2-} (b), NO_3^- (c), HCO_3^- (d), HA (e) to the $\text{Ca}(\text{OH})_2/\text{PMS}$ system, $[\text{Ca}(\text{OH})_2]_0 = 1 \text{ mM}$, $[\text{PMS}]_0 = 1.5 \text{ mM}$, $[\text{BPS}]_0 = 20 \mu\text{M}$.



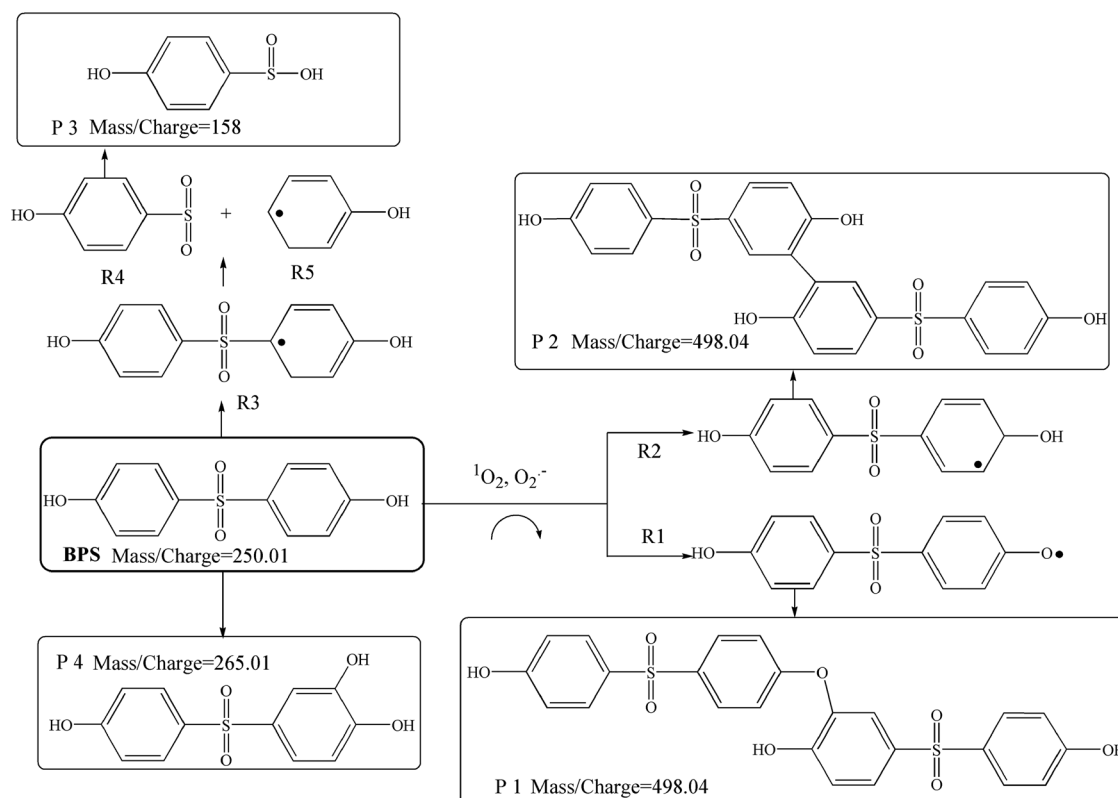
Fig. 6 Removal of PMS (a), BPS and TOC (b) in the $\text{Ca}(\text{OH})_2/\text{PMS}$ system.

However, the TOC removal percentage of the $\text{Ca}(\text{OH})_2/\text{PMS}$ system was only 17.52% within 240 min (Fig. 6(b)), which indicated incomplete mineralization of BPS and presence of intermediate products. A total of 4 degradation products of BPS were identified by LC-TOF-MS. According to these intermediates, 3 possible transformation pathways were proposed as shown in Fig. 7. ^1O_2 and $\text{O}_2^{\cdot-}$ initially attacked the phenol moiety of BPS and acquired one electron, and then transformed into some phenoxy radical (R1) and other resonance forms (R2 and R3) due to the delocalization of the unpaired electron.² R1 and R2 could react with each other and generate resultant dimers (P1 and P2) by C-C and C-O coupling.² The radicals (R3)

with high electron density at the para position would generate R4 and R5 via β -scission reaction. Then, 4-hydroxybenzenesulfonic acid (P3) would be formed from the hydroxylation of R4.⁴⁴ In the other way, the resonance form (R2) was hydroxylated directly to formed P4.

3.8 Influence of different water matrices

The influence of different water matrices including ultrapure water, Poyang lake water, Yaohu lake water and domestic wastewater on BPS degradation in the $\text{Ca}(\text{OH})_2/\text{PMS}$ system were investigated. As illustrated in Fig. 8(a), 100% BPS removal was achieved in the ultrapure water, but it was slightly inhibited

Fig. 7 Possible degradation pathways of BPS in the $\text{Ca}(\text{OH})_2/\text{PMS}$ system.

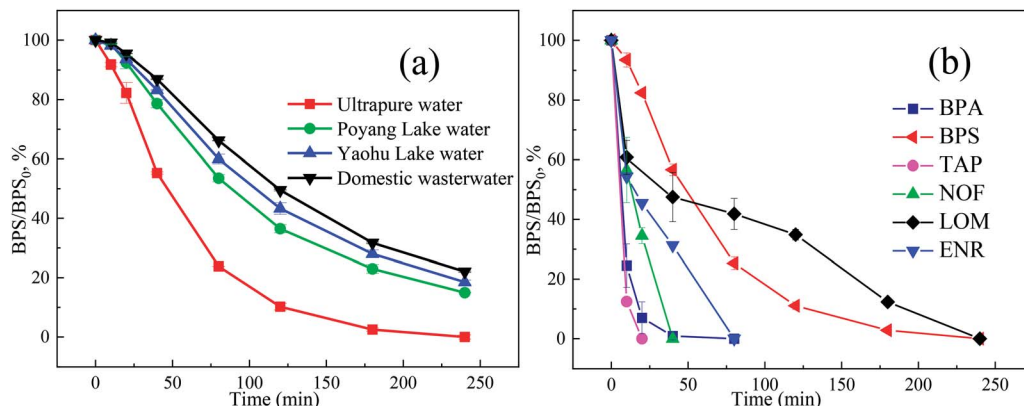


Fig. 8 The reaction in different water matrices (a), the degradation of different pollutants in the $\text{Ca}(\text{OH})_2/\text{PMS}$ system (b), $[\text{Ca}(\text{OH})_2]_0 = 1 \text{ mM}$, $[\text{PMS}]_0 = 1.5 \text{ mM}$, $[\text{BPS}]_0 = 20 \mu\text{M}$.

in Poyang Lake water (81.48%), Yaohu Lake water (77.94%) and domestic wastewater (75.86%). Accordingly, the k_{obs} values of BPS removal were decreased to 0.00730 min^{-1} , 0.00660 min^{-1} and 0.00630 min^{-1} , respectively. Based on the detailed physicochemical properties of real water samples (Table S1†) and the results about co-existing anions and HA from Section 3.7. This phenomenon could attribute to the fact that real water matrices were rich in NOM, which may act as ROS scavenger, further affect the degradation of BPS.

3.9 Wide applicability of the $\text{Ca}(\text{OH})_2/\text{PMS}$ system

Apart from BPS, the performances of the $\text{Ca}(\text{OH})_2/\text{PMS}$ system were also evaluated by degrading several typical organic pollutants, including antibiotics (TAP, NOF, LOM, and ENR), and endocrine disruptor (BPA) at $20 \mu\text{M}$ (Fig. 8(b)). Just like the removal of BPS in the $\text{Ca}(\text{OH})_2/\text{PMS}$ system, the whole of TAP, NOF, BPA, ENR and LOM could be removed within 20 min, 40 min, 80 min, 80 min and 240 min, respectively. ${}^1\text{O}_2$ could oxidize electron-rich compounds (electron-rich phenols, olefins, and sulfides),⁴⁵ therefore, the $\text{Ca}(\text{OH})_2/\text{PMS}$ system can be widely used to degrade a variety of organic pollutants. However, the specific degradation mechanism needs further exploration.

4 Conclusions

In the present study, the enhanced effect of the $\text{Ca}(\text{OH})_2$ on BPS removal by the $\text{Ca}(\text{OH})_2/\text{PMS}$ system was observed. 100% BPS were efficiently removed in a certain condition ($[\text{Ca}(\text{OH})_2]_0 = 1 \text{ mM}$, $[\text{PMS}]_0 = 1.5 \text{ mM}$). The degradation of BPS maintained on a high level in a wide range of pH values and optimized alkali activated PMS making the final pH close to neutral. BPS degradation was significantly accelerated with the temperature increased. The adding mode of PMS implied that the higher initial PMS concentration led to the higher BPS degradation. The SO_4^{2-} , NO_3^- had no significant influence on BPS degradation, however, the HCO_3^- and HA inhibited the BPS oxidation. Cl^- had a dual effect on BPS degradation, a low concentration of Cl^- will inhibit the degradation of BPS, but a higher

concentration of Cl^- would promote the degradation of BPS due to the generation of reactive chlorine. Based on the quenching experiments, it was indicated that both O_2^- and ${}^1\text{O}_2$ have participated in the $\text{Ca}(\text{OH})_2/\text{PMS}$ system, and ${}^1\text{O}_2$ played a major role on BPS degradation. Only 17.52% of TOC were removed, which indicated the incomplete mineralization of BPS and the presence of intermediate products. A total of 4 degradation intermediates of BPS were identified and possible transformation pathways were proposed. BPS degradation efficiency in the real waters was lower than that in ultrapure water due to the presence of matrixes. Furthermore, other pollutants including (TAP, NOF, LOM and ENR) exhibited an efficient degradation in the $\text{Ca}(\text{OH})_2/\text{PMS}$ system.

Author contributions

Leliang Wu: writing, methodology, conceptualization, validation. Yiting Lin: methodology, validation. Yimin Zhang: methodology. Peng Wang: supervision. Mingjun Ding: supervision. Minghua Nie: ideas, supervision, conceptualization, investigation, writing – review & editing. Caixia Yan: investigation, writing – review & editing, supervision.

Conflicts of interest

The authors declare that they have no known competing financial interests or personal relationships that could have appeared to influence the work reported in this paper.

Acknowledgements

This work was financially supported by the National Natural Science Foundation of China (No. 42067034, 42067058), the Jiangxi Provincial Natural Science Foundation (20202BAB203015, 20202BAB203014), and the Open Fund of Key Laboratory of Eco-geochemistry, Ministry of Natural Resources (ZSDHJJ202004).



References

1 T. B. Nguyen and R. Doong, Heterostructure $\text{ZnFe}_2\text{O}_4/\text{TiO}_2$ nanocomposites with a highly recyclable visible-light-response for bisphenol A degradation, *RSC Adv.*, 2017, **7**, 50006–50016.

2 T. Yang, L. Wang, Y. Liu, Z. Huang, H. He, X. Wang, J. Jiang, D. Gao and J. Ma, Comparative study on ferrate oxidation of BPS and BPAF: kinetics, reaction mechanism, and the improvement on their biodegradability, *Water Res.*, 2019, **148**, 115–125.

3 L. Li, D. Xu and Z. Pei, Kinetics and thermodynamics studies for bisphenol S adsorption on reduced graphene oxide, *RSC Adv.*, 2016, **6**, 60145–60151.

4 S. Kitamura, T. Suzuki, S. Sanoh, R. Kohta, N. Jinno, K. Sugihara, S. Yoshihara, N. Fujimoto, H. Watanabe and S. Ohta, Comparative study of the endocrine-disrupting activity of bisphenol A and 19 related compounds, *Toxicol. Sci.*, 2005, **84**, 249–258.

5 S. B. Hammouda, F. Zhao, Z. Safaei, D. L. Ramasamy, B. Doshi and M. Sillanpaa, Sulfate radical-mediated degradation and mineralization of bisphenol F in neutral medium by the novel magnetic $\text{Sr}_2\text{CoFeO}_6$ double perovskite oxide catalyzed peroxymonosulfate: influence of co-existing chemicals and UV irradiation, *Appl. Catal., B*, 2018, **233**, 99–111.

6 Z. Fang, Y. Gao, X. Wu, X. Xu, A. K. Sarmah, N. Bolan, B. Gao, S. M. Shaheen, J. Rinklebe, Y. S. Ok, S. Xu and H. Wang, A critical review on remediation of bisphenol S (BPS) contaminated water: Efficacy and mechanisms, *Environ. Sci. Technol.*, 2020, **50**, 476–522.

7 F. Ghanbari and M. Moradi, Application of peroxymonosulfate and its activation methods for degradation of environmental organic pollutants, *Chem. Eng. J.*, 2017, **310**, 41–62.

8 W. Tang, Y. Zhang, H. Guo and Y. Liu, Heterogeneous activation of peroxymonosulfate for bisphenol AF degradation with $\text{BiOI}_{0.5}\text{Cl}_{0.5}$, *RSC Adv.*, 2019, **9**, 14060.

9 Y. Li, Y. Shi, D. Huang, Y. Wu and W. Dong, Enhanced activation of persulfate by Fe (III) and catechin without light: Reaction kinetics, parameters and mechanism, *J. Hazard. Mater.*, 2021, **413**, 125420.

10 M. Nie, W. Zhang, C. Yan, W. Xu, L. Wu, Y. Ye, Y. Hu and W. Dong, Enhanced removal of organic contaminants in water by the combination of peroxymonosulfate and carbonate, *Sci. Total Environ.*, 2019, **647**, 734–743.

11 C. Qi, X. Liu, J. Ma, C. Lin, X. Li and H. Zhang, Activation of peroxymonosulfate by base: Implications for the degradation of organic pollutants, *Chemosphere*, 2016, **151**, 280–288.

12 J. Zhang, X. Shao, C. Shi and S. Yang, Decolorization of acid orange 7 with peroxymonosulfate oxidation catalyzed by granular activated carbon, *Chem. Eng. J.*, 2013, **232**, 259–265.

13 X. Zhou, A. Jawad, M. Luo, C. Luo, T. Zhang, H. Wang, J. Wang, S. Wang, Z. Chen and Z. Chen, Regulating activation pathway of Cu/persulfate through the incorporation of unreduceable metal oxides: Pivotal role of surface oxygen vacancies, *Appl. Catal., B*, 2021, **286**, 119914.

14 H. Lee, H. J. Lee, J. Jeong, J. Lee, N. B. Park and C. Lee, Activation of persulfates by carbon nanotubes: oxidation of organic compounds by nonradical mechanism, *Chem. Eng. J.*, 2015, **266**, 28–33.

15 Y. Zhou, Y. Gao, J. Jiang, Y. Shen, S. Pang, Z. Wang, J. Duan, Q. Guo, C. Guan and J. Ma, Transformation of tetracycline antibiotics during water treatment with non-activated peroxymonosulfate, *Chem. Eng. J.*, 2020, **379**, 122378.

16 Y. Guan, J. Ma, Y. Ren, Y. Liu, J. Xiao, L. Lin and C. Zhang, Efficient degradation of atrazine by magnetic porous copper ferrite catalyzed peroxymonosulfate oxidation via the formation of hydroxyl and sulfate radicals, *Water Res.*, 2013, **47**, 5431–5438.

17 A. D. Bokare, R. C. Chikate, C. V. Rode and K. M. Paknikar, Effect of surface chemistry of Fe-Ni nanoparticles on mechanistic pathways of azo dye degradation, *Environ. Sci. Technol.*, 2007, **41**, 7437–7443.

18 W. Wu, S. Zhu, X. Huang, W. Wei and B. Ni, Mechanisms of persulfate activation on biochar derived from two different sludges: dominance of their intrinsic compositions, *J. Hazard. Mater.*, 2021, **408**, 124454.

19 Y. Zhou, J. Jiang, Y. Gao, J. Ma, S. Pang, J. Li, X. Lu and L. Yuan, Activation of peroxymonosulfate by benzoquinone: a novel nonradical oxidation process, *Environ. Sci. Technol.*, 2015, **49**, 12941–12950.

20 Y. Peng, H. Tang, B. Yao, X. Gao, X. Yang and Y. Zhou, Activation of peroxymonosulfate (PMS) by spinel ferrite and their composites in degradation of organic pollutants: A Review, *Chem. Eng. J.*, 2021, **414**, 128800.

21 X. Lou, C. Fang, Z. Geng, Y. Jin, D. Xiao, Z. Wang, J. Liu and Y. Guo, Significantly enhanced base activation of peroxymonosulfate by polyphosphates: Kinetics and mechanism, *Chemosphere*, 2017, **173**, 529–534.

22 E. Baralla, V. Pasciu, M. V. Varoni, M. Nieddu, R. Demuro and M. P. Demontis, Bisphenols' occurrence in bivalves as sentinel of environmental contamination, *Sci. Total Environ.*, 2021, **785**, 147263.

23 J. Deng, S. Feng, K. Zhang, J. Li, H. Wang, T. Zhang and X. Ma, Heterogeneous activation of peroxymonosulfate using ordered mesoporous Co_3O_4 for the degradation of chloramphenicol at neutral pH, *Chem. Eng. J.*, 2017, **308**, 505–515.

24 J. Tang, L. Tang, H. Feng, G. Zeng, H. Dong, C. Zhang, B. Huang, Y. Deng, J. Wang and Y. Zhou, pH-dependent degradation of p-nitrophenol by sulfidated nanoscale zerovalent iron under aerobic or anoxic conditions, *J. Hazard. Mater.*, 2016, **320**, 581–590.

25 J. Yu, J. Zhang, T. Zeng, H. Wang, Y. Sun, L. Chen, S. Song and H. Shi, Stable incorporation of MnO_x quantum dots into N-doped hollow carbon: a synergistic peroxymonosulfate activator for enhanced removal of bisphenol A, *Sep. Purif. Technol.*, 2019, **213**, 264–275.

26 F. Ghanbari, M. Ahmadi and F. Gohari, Heterogeneous activation of peroxymonosulfate via nanocomposite $\text{CeO}_2\text{-Fe}_3\text{O}_4$ for organic pollutants removal: the effect of UV and



US irradiation and application for real wastewater, *Sep. Purif. Technol.*, 2019, **228**, 115732.

27 S. H. Do, J. H. Jo, Y. H. Jo, H. K. Lee and S. H. Kong, Application of a peroxyomonosulfate/cobalt (PMS/Co (II)) system to treat diesel-contaminated soil, *Chemosphere*, 2009, **77**, 1127–1131.

28 M. Nie, Y. Yang, Z. Zhang, C. Yan, X. Wang, H. Li and W. Dong, Degradation of chloramphenicol by thermally activated persulfate in aqueous solution, *Chem. Eng. J.*, 2014, **246**, 373–382.

29 S. Wang, J. Tian, Q. Wang, F. Xiao, S. Gao, W. Shi and F. Cui, Development of CuO coated ceramic hollow fiber membrane for peroxyomonosulfate activation: a highly efficient singlet oxygen-dominated oxidation process for bisphenol a degradation, *Appl. Catal., B*, 2019, **256**, 117783.

30 J. A. Khan, X. He, H. M. Khan, N. S. Shah and D. D. Dionysiou, Oxidative degradation of atrazine in aqueous solution by UV/H₂O₂/Fe²⁺, UV/Fe²⁺ and UV/Fe²⁺ processes: a comparative study, *Chem. Eng. J.*, 2013, **218**, 376–383.

31 J. Deng, Y. Shao, N. Gao, Y. Deng, S. Zhou and X. Hu, Thermally activated persulfate (TAP) oxidation of antiepileptic drug carbamazepine in water, *Chem. Eng. J.*, 2013, **228**, 765–771.

32 L. Zhang, J. Chen, W. Li, Z. Wang and T. Huang, Kinetics for degradation of Orange G with peroxyomonosulfate activated by carbon nanotubes, *Environ. Sci. Technol.*, 2016, **37**, 2601–2609.

33 J. Yan, J. Li, J. Peng, H. Zhang and B. Lai, Efficient degradation of sulfamethoxazole by the CuO@Al₂O₃ (EPC) coupled PMS system: optimization, degradation pathways and toxicity evaluation, *Chem. Eng. J.*, 2019, **359**, 1097–1110.

34 G. Peng, W. You, W. Zhou, G. Zhou, C. Qi and Y. Hu, Activation of peroxyomonosulfate by phosphite: kinetics and mechanism for the removal of organic pollutants, *Chemosphere*, 2021, **266**, 129016.

35 G. Lente, J. Kalmar, Z. Baranyai, A. Kun, I. Kek, D. Bajusz, M. Takacs, L. Veres and I. Fabian, One-versus two-electron oxidation with peroxyomonosulfate ion: reactions with iron (II), vanadium (IV), halide ions, and photoreaction with cerium (III), *Inorg. Chem.*, 2009, **48**, 1763–1773.

36 G. Peng, T. Li, B. Ai, S. Yang, J. Fu, Q. He, G. Yu and S. Deng, Highly efficient removal of enrofloxacin by magnetic montmorillonite *via* adsorption and persulfate oxidation, *Chem. Eng. J.*, 2019, **360**, 1119–1127.

37 L. Xu, R. Yuan, Y. Guo, D. Xiao, Y. Cao, Z. Wang and J. Liu, Sulfate radical-induced degradation of 2,4,6-trichlorophenol: a de novo formation of chlorinated compounds, *Chem. Eng. J.*, 2013, **217**, 169–173.

38 R. Yuan, S. N. Ramjaun, Z. Wang and J. Liu, Effects of chloride ion on degradation of acid orange 7 by sulfate radical-based advanced oxidation process: implications for formation of chlorinated aromatic compounds, *J. Hazard. Mater.*, 2011, **196**, 173–179.

39 Z. Huang, Y. Yao, J. Lu, C. Chen, W. Lu, S. Huang and W. Chen, The consortium of heterogeneous cobalt phthalocyanine catalyst and bicarbonate ion as a novel platform for contaminants elimination based on peroxyomonosulfate activation, *J. Hazard. Mater.*, 2016, **301**, 214–221.

40 Y. Peng, H. Shi, Z. Wang, Y. Fu and Y. Liu, Kinetics and reaction mechanism of photochemical degradation of diclofenac by UV-activated peroxyomonosulfate, *RSC Adv.*, 2021, **11**, 6804.

41 Z. Fang, J. Zhao, Y. Li, Y. Wang, T. Qiu, Y. Wu, W. Dong and G. Mailhot, Improving Fenton-like system with catechin, an environmental-friendly polyphenol: effects and mechanism, *Chem. Eng. J.*, 2021, **426**, 127946.

42 S. Tang, J. Tang, D. Yuan, Z. Wang, Y. Zhang and Y. Rao, Elimination of humic acid in water: comparison of UV/PDS and UV/PMS, *RSC Adv.*, 2020, **10**, 17627–17634.

43 L. Chen, D. Ding, C. Liu, H. Cai, Y. Qu, S. Yang, Y. Gao and T. Cai, Degradation of norfloxacin by CoFe₂O₄-GO composite coupled with peroxyomonosulfate: a comparative study and mechanistic consideration, *Chem. Eng. J.*, 2018, **334**, 273–284.

44 J. Peng, H. Zhou, W. Liu, Z. Ao, H. Ji, Y. Liu, S. Su, G. Yao and B. Lai, Insights into heterogeneous catalytic activation of peroxyomonosulfate by natural chalcopyrite: pH-dependent radical generation, degradation pathway and mechanism, *Chem. Eng. J.*, 2020, **397**, 125387.

45 H. Kim, W. Kim, Y. Mackeyev, G. Lee, J. Kim, T. Tachikawa, S. Hong, S. Lee, J. Kim, L. Wilson, T. Majima, P. Alvarez, W. Choi and J. Lee, Selective oxidative degradation of organic pollutants by singlet oxygen-mediated photosensitization: Tin porphyrin *versus* C₆₀ amino fullerene systems, *Environ. Sci. Technol.*, 2012, **46**, 9606–9613.

